SUPPLEMENTARY MATERIAL TABLE OF CONTENTS

SUPPLEMENTARY METHODS

Animal Models:

Genetic Model: Experiments were carried out in accordance with local and NIH guidelines, and the animal protocol was approved by the University of Virgina and University of Rochester Institutional Animal Care and Use Committee. All mice were maintained on a 12-hour light-dark cycle with free access to standard chow and water. Animals were ~8 weeks old at the start of experiments unless otherwise specified. The mouse line carrying the *Gstm1* deletion was generated by the electroporation of embryonic stem cells derived from the 129/SvEv (129S6, Taconic) strain with a targeting construct to disrupt a 20 kb segment of the *Gstm1* locus (**Supplementary Fig. 1A**). Genotyping was performed using an RT-PCR protocol with primers that recognize the *Gstm1* exon 5 (forward: 5'-CAC AAA GTC AGG GTT GTA ACA GAG C-3', and reverse: 5'-GTT GGG ATG CCT AGT GTA CTG TG-3'). Ablation of *Gstm1* was confirmed by Southern blot and RT-qPCR (**Supplementary Fig. 1B-C**).

Nx-CKD Model: A sub-total nephrectomy (Nx) was used to induce CKD in the model, as previously described (1). Briefly, mice were anesthetized with 2-4% isoflurane. The right kidney was removed and the cranial branch of the left renal artery was ligated, resulting in the infarction of the cranial pole of the left kidney. Mice were allowed to recover for at least 4 weeks before being subjected to any other procedures.

AngII-HTN Model: The HTN model was induced by the delivery of angiotensin II (AngII, Sigma-Aldrich, St. Luis, MO) at 1000 ng/kg/min over 4 weeks via Alzet mini-osmotic pumps (Durect Corporation, Cupertino, CA, model 2004). The pumps were implanted subcutaneously in the back near the left hind limb.

Dietary Interventions: AngII-HTN mice that were treated with Tempol (4-Hydroxy-Tempo, Sigma-Aldrich, St. Luis, MO) had 3 mmol/L Tempol added to their drinking water during the

entire period of AngII infusion. Mice treated with sulforaphane rich broccoli powder (SRBP, Natural Sprout Company, LLC) had it mixed with powdered chow at a 1:1 ratio. SRBP does not contain sulforaphane, but rather glucoraphanin, that is metabolized into sulforaphane in the gut. The manufacturer indicated that the SRBP contained an equivalent of 3.5-4.0 mg sulforaphane/g of SRBP. We estimate that mice were receiving a dose of about 250 mg/kg/d and getting a peak concentration of sulforaphane in the blood equivalent to that of a bolus dose of ~50 mg/kg, based on first-order pharmacokinetics (2).

***Blood pressure monitoring* in vivo**:

Radiotelemetry: Blood pressure was measured in conscious mice under unrestrained conditions by radiotelemetry (TA11PA-C10, Data Sciences International, St. Paul, MN), as previously described (3). Briefly, mice were anesthetized with 2-4% isoflurane and had the radiotelemetry catheter implanted into the left carotid artery. A subcutaneous pouch was made along the right flank of the animal, and the transmitter was placed as caudally as possible. Mice were housed in individual cages on receivers and allowed to recover for at least 7 days after implantation of the radiotelemetry device before meausrements were recorded and analyzed using Dataquest A.R.T. 20 software (Data Sciences International). Implantation was performed at least 4 weeks after Nx-CKD or before AngII-HTN initiation. Reported values are mean ± SD.

Tail-cuff manometry (performed in 1 year old un-manipulated WT and KO mice: Mice were trained daily for blood pressure measurement using a computerized tail-cuff (Hatteras Instruments, Cary NC) as described previously. SBPs were recorded at least 5 days a week, 10-20 measurements each day, for two weeks. Results are expressed as mean SBP over the two week period.

Urine measurements: Urine samples were collected over 24 h from mice placed in individual metabolic cages for assessment of 8-isoprostane, urinary albumin and creatinine as previously

described (1). Urinary isoprostane was measured using the ELISA kit from Oxford Biomedical Research (Oxford, MI). Urinary albumin and creatinine were measured using the Albuwell M Murine ELISA kit, and Creatinine Companion kit (Exocell, Philadelphia PA).

Measurement of tissue superoxide: The Lucigenin assay was modified from previous studies as described (3). Kidney cortical tissue (3-5 mg) was incubated for 5 min @ 37°C in 5 µM Lucigenin (9,9'-Bis-N-methylacridinium nitrate, Sigma: M8010) solution prepared in Krebs-Hepes buffer. Luminescence counts were taken 5 times for 1 minute each, averaged, corrected for background and normalized to dry tissue weight

Histopathologic analyses: Tissue was fixed in 10% neutral-buffered formalin, embedded in paraffin, sectioned and stained with periodic acid-Schiff (PAS). Kidney injury was scored in the glomeruli, tubules, and interstitium compartments as previously described (1) by a renal immunopathologist (P.R.) blinded to mouse genotypes and experimental conditions. Digital quantitation of glomerular and mesangial surface areas was performed by light microscopy (Zeiss Axio Imager Z2) using Stereoinvestigator software (BMF Bioscience) as previously described (4).

Podocyte isolation and scratch assay: Podocytes were isolated as previously described (5). Primary podocytes reached confluence ~7-9 days after glomeruli isolation. At confluence, mechanical scraping was performed with a 200 µL pipette tip, creating a rectangular-shaped wound in the podocyte layer from one edge of the well to the opposite. Images of podocytes with the scratched area were taken immediately after wound creation (0 h) and after 14 h using an EVOS XL Core Cell Imaging System at 10x magnification. The images were analyzed using ImageJ software (1.48v, NIH, USA) to obtain pixel counts in the scratched area void of podocytes.

***Gene expression analysis*:** RNA from frozen kidney tissue was isolated by RNeasy Mini kit (Qiagen) and transcribed to cDNA by iScript cDNA synthesis kit (Bio-Rad). Real-time RT-PCR analysis was performed on an iQ5 multicolor real-time system (Bio-Rad) using iQ SYBER Green Supermix. *Hprt* was used as the reference gene for normalization. The sequences of all primers used in this study are listed in **Supplementary Table 12**.

***Flow cytometry*:** Kidney tissue was isolated and homogenized in RPMI media and then incubated with collagenase (1 mg/mL) and DNase I (100 µL (20X)) for 25 minutes at 37ºC in 1X PBS. 5 mL of PBS was added and samples were centrifuged at 400 g (4ºC) for 8 min. Each sample was then filtered through 32 µm filter to collect kidney single cell suspension. Samples were again centrifuged and 100 µL aliquots of each sample were used for staining. Antibody mixes were performed using final concentrations ranging from 4 to 20 µg/mL. Samples were incubated with appropriate antibody mixes for 1 hour at 4ºC, diluted with 200 µL of 1X PBS-0.1% sodium Azide solution and analyzed immediately on a BD FACSCalibur (BD Biosciences, San Jose, CA) with Cytek eightcolor flow cytometry upgrade (Cytek Development, Fremont, CA). Live cells from the whole kidney single-cell suspension were first selected based on low positive staining for the live/dead marker 7AAD that binds to DNA only in dead cells. This live (7AAD negative) population was then further refined for single cells (discriminating against doublets) based on FSC-A / FSC-W gating. The live, singlet population (over 1 million cells) was then assayed for CD45 positivity, resulting in 5,000-30,000 CD45$^+$ cells (leukocytes) being quantified per sample. The resultant cell populations were then identified and quantified based on positivity for respective markers for CD4$^+$ T cells, CD8$^+$ T cells, B cells, polymorphonuclear neutrophils (PMN) and macrophages (F4/80). All demarcations for gating positive-negative populations were based on single-stained controls. The gating strategy is shown in **Supplementary Fig 4.**

Immunostaining and Confocal Microscopy: Kidney sections were fixed in 2% p-formaldehyde-lysine-periodate (PLP) for 3 h and equilibrated in sucrose as previously described (6). Tissue sections of 5 µm thickness were stained by fluorochrome-conjugated antibodies. Only antibodies directly conjugated with Alexa Fluors were used in tissue staining because secondary staining reagents gave high non-specific background. Fluorochrome-labeled isotype control antibody showed no background staining above tubule autofluorescence in confocal microscopy. Four-color confocal images were captured on a Zeiss LSM-700 confocal microscope equipped with 405, 488, 561 and 633 nm laser lines at the University of Virginia Advanced Microscopy Center and analyzed by the program ZEN (Zeiss, Thornwood, NY). Rat or hamster monoclonal antibodies against the following antigens with or without fluorochrome conjugation were from Biolegend (San Diego, CA): CD11b (M1/70), F4/80 (CI:A3-1), and I-A/I-E (M5/114.15.2). Affinity-purified polyclonal antibody against recombinant mouse Itgα8 protein was from R&D (Minneapolis, MN, USA). For fluorescence in the 561 nm and 633 nm channels, antibodies were conjugated with Alexa Fluor 555 and Alexa Fluor 647 monoclonal antibody labeling kits (Invitrogen), respectively.

Bone marrow cross-transplantation: Recipient animals at 6-7 weeks of age were placed in the irradiator in the animal vivarium for 2 does of 650 rads each, 4 h apart. Within 4 h after the second dose of irradiation, bone marrow (BM) cells were obtained from a donor mouse by flushing the cells from the femurs and tibias suspended in sterilized saline through a 25 µm cell strainer. Cells were then centrifuged at 1000 rpm for 5 min. The supernatant was discarded and the pellet was re-suspended in 200 µL of sterilized saline. The recipient mouse was confined in a plexiglass tube, had its tail vein briefly dipped in warm water to dilate the blood vessels, and then had 0.2 mL of the BM cell suspension (5 million cells) injected into the tail vein with a small gauge needle. To prevent infection, recipient mice were given autoclaved food and water with on antibiotics in the water (7.5 mL of 20 mg/mL Baytril in 350 mL water) for 5 weeks. After 8

weeks, recipient mice were subjected to the AngII-HTN model as described above. Crosstransplantation of all 4 possible combinations of recipient and donor animals were performed.

***Tautomerase activity*:** Tautomerase activity of the macrophage migration inhibitory factor (MIF) was used as a biomarker for MIF inhibition. Tautomerase activity was assayed as previously described (7), modified to measure activity in tissue lysates. Briefly, substrate (8) was prepared by mixing equal volumes of 4 mmol/L L-3,4-Dihydroxyphenylalanine methyl ester hydrochloride (dopachrome, Sigma) and 8 mmol/L sodium (meta)periodate (Sigma) and incubated at room temperature for 5 min. Tissue lysates were normalized for total protein, and tautomerase activity was assayed in 25 mmol/L phosphate buffer (pH 6.0)/1 mmol/L EDTA buffer containing 100 µL/mL freshly prepared substrate. Decolorization was monitored over time by OD at 475 nm. For this assay, synthetic sulforaphane (Lkt Labs) was administered to WT mice in a single 2 mg intraperitoneal (IP) injection and compared to mice receiving a 1:1 mix of SRBP in chow as detailed above.

***Statistical analysis for animal studies*:** Student's unpaired *t*-test, one-way ANOVA with post-hoc Bonferroni correction and 2-way ANOVA were used as indicated. Differences in Kaplan-Meier survival curves were tested using the log-rank test. Differences were considered statistically significant when $p < 0.05$.

ARIC study

The ARIC study is a prospective cohort study of 15,792 participants, aged 45 to 65 at visit 1 (1987-89) from four US communities with Jackson, MS consisting of exclusively African-American participants and the other three sites enrolled almost exclusively European Americans (Forsyth, NC; suburbs of Minnespolis, MN; Washington county, MD) (9). Of the 11,893 participants with exome sequencing, we excluded those with exome sequencing reads that did

not pass quality filters (see below, n = 218), missing baseline (visit 1) cruciferous vegetable intake assessment (n = 257), eGFR < 15 mL/min/1.73 m^2 or missing eGFR (n = 101), missing kidney failure outcome or genetic principal components (n = 256), missing clinical covariates (n = 314), self-reported African Americans from the Minneapolis and Washington county sites (n = 2) and participants who were considered related based on genetic distance and principal component analysis (n = 590). The overall analyzed sample for this study included 10,155 participants. The included participants provided informed consent for genetic studies. This study has been approved by the Johns Hopkins Institutional Review Board.

Assessment of cruciferous vegetable intake in ARIC

Details of dietary assessment have been reported previously (10). Briefly, prior to the clinical examination, participants were mailed a food frequency questionnaire (FFQ) on their dietary intake in the previous year (the Willett 131-item food frequency questionnaire) (11). Participants self-administered the FFQ in their homes and brought the completed surveys to their scheduled clinical examination where clinic staff briefly reviewed the FFQ with the participants to assure completeness. Prior to scanning, forms were reviewed a second time. If missing responses were found, the participant was contacted by the field center staff to provide values for the missing response, if possible.

The frequency of cruciferous vegetable intake was collected from two questions: one on broccoli intake and the other on cabbage, cauliflower and Brussels sprouts intake. These vegetables have commonly been considered as cruciferous vegetables containing ITC, a class of protective electrophiles (12). The frequency of intake was ascertained in nine categories from "almost never" to "> 6 times per day" for a serving size of 0.5 cup (**Supplementary Table 10**). In the current study, each serving (0.5 cup) of broccoli, cabbage, cauliflower or Brussels sprouts was considered as one serving of cruciferous vegetable. Based on previous findings on the influence of *GSTM1* genotype on the protective effect of cruciferous vegetable intake on lung

cancer (13) and ensuring that the number of kidney failure cases was not too small after stratifying by race, *GSTM1* genotype and cruciferous vegetable intake levels (**Supplementary Table 11**) we categorized cruciferous vegetable intake into three levels: low (≤ 3 times per month), medium (> 3 times per month to < once per week), high (≥ once per week).

Definitions of kidney failure in ARIC

Kidney failure was defined as ESRD ascertained using linkage to the U.S. Renal Data System (USRDS) or kidney failure based on International Classification of Diseases, Ninth or Tenth Revision, Clinical Modification (ICD-9-CM/ICD-10-CM) code for hospitalization or death (14). Based on the review of 546 charts by trained physicians, the sensitivity and specificity of kidney failure based on ICD code were 88% and 97%, respectively, and those of ESRD were 95% and 100%, respectively. Participants were followed from the baseline (visit 1) to December 2013.

Determination of GSTM1 genotype in ARIC

The methods for determining *GSTM1* genotype using exome sequencing reads have been reported previously (15). Briefly, the CODEX R package was used to read in the exome sequencing data with the following quality control filters: coverage > 4000 reads, mappability < 0.4, GC content < 0.20 or > 0.80 and mapping quality < 20 (16). We further excluded overall median coverage at chromosome 1 < 40 reads and read lengths with less than 5 samples. Next, we normalized the coverage at each exon of *GSTM1* using the mean coverage of all captured regions at chromosome 1 containing *GSTM1*. To combine all available information at *GSTM1*, we summed the normalized coverage of all eight exons of *GSTM1*. Since read length affects coverage distribution, sums of the normalized coverage were grouped by read length ranging from 50 base pairs to 101 base pairs. Based on the distribution of the sum of the normalized coverage, we determined empirical thresholds for determining *GSTM1* deletion. **Supplementary Figure 6A** presents the histogram of the sum of the normalized coverage in each read length with the empirical thresholds.

We validated this algorithm using exome sequencing reads against the results from real-time PCR. Based on a power calculation for detecting concordance of ≥ 0.8 using the R package kappaSize, a random sample of 224 participants with exome sequencing reads were selected with approximately the same number of participants in each genotype (African Americans: *GSTM1*(0/0) 35; *GSTM1*(0/1) 36; *GSTM1*(1/1) 36; European Americans: *GSTM1*(0/0) 39; *GSTM1*(0/1) 39; *GSTM1*(1/1) 39). Lab personnel who performed the real-time PCR were blinded to the *GSTM1* deletion genotype based on exome sequencing reads. The real-time PCR were run in triplicate with *RPPH1*, a housekeeping gene, and *GSTM1* on the same well for the samples of the same participant. For *RPPH1*, samples with a cycle threshold (Ct) value > 35 were considered having amplification problems and were removed. We calculated the difference in Ct (ΔCt) between *GSTM1* and *RPPH1* in the same well and the standard deviation (SD) among the ΔCts for each participant. We identified participants with outliers using a threshold of > 0.4 in ΔCt SD based on the distribution of the SD. The outliers for each participant were removed. To determine *GSTM1* deletion genotype from the real-time PCR experiment, we used the following algorithms: if a participant had at least two samples that failed to amplify *GSTM1* and two samples that amplified *RPPH1*, the participant was considered as homozygous deletion. For heterozygous deletion and no deletion, we calculated the mean of the ΔCts of each participant, plotted the distributions of the mean ΔCt by plate and selected break points that separate heterozygous deletion versus no deletion (**Supplementary Figure 6B**). Twelve participants were removed due to having < 2 ΔCt after removing outliers or *RPPH1* Ct > *35* (212 participants used in analysis). The resulting concordance of the deletion genotype between using real-time PCR and exome sequencing was 93% (**Supplementary Figure 6C**)**.**

GSTM1 genetic models in ARIC

We adopted the recessive genetic model, i.e. homozygous deletion (*GSTM1*(0/0)) vs. heterozygous deletion (*GSTM1*(0/1) and no deletion (*GSTM1*(1/1)) combined, as our primary

model based on previous findings from lung cancer in humans (13, 17-19). We also performed secondary analysis using the genotypic model, i.e. using the three genotypes as a categorical variable.

Measures of covariates in ARIC

Race, smoking status, and education levels were based on self-report. Diabetes was defined as the use of diabetes medication, a fasting glucose level ≥ 126 mg/dL, a random glucose ≥ 200 mg/dL or self-reported physician diagnosis of diabetes. Prevalent HTN was defined as SBP ≥ 140 mmHg, diastolic blood pressure ≥ 90 mmHg or the use of antihypertensive medication for controlling blood pressure. Prevalent coronary heart disease was defined as self-reported myocardial infarction (MI) or cardiac procedure or electrocardiogram evidence of a prior MI. Chronic Kidney Disease Epidemiology Collaboration (CKD-EPI) creatinine equation was used to calculate eGFR (20). Physical activity was assessed by the Baecke questionnaire (21). Total calorie intake was calculated by multiplying the frequency of consumption of specified unit or portion size of food by its nutrient content and summing across all foods. Genetic principal components for controlling population stratification were generated using genotypes from the Illumina Human Exome BeadChip after quality control (22).

Statistical Analysis in the ARIC study

We compared the baseline characteristics of participants by three levels of cruciferous vegetable intake using t-tests for non-skewed continuous variables, Wilcoxon tests for skewed continuous variables, and chi-squared tests as appropriate. Our primary analysis evaluated the association between the three levels of cruciferous vegetable intake and kidney failure stratified by *GSTM1* homozygous deletion to determine whether the protective effect of cruciferous vegetable intake was indeed stronger among participants with *GSTM1*(0/0). Kaplan-Meier curves were plotted by the three levels of cruciferous vegetable intake by *GSTM1* homozygous deletion. Risk of kidney failure was assessed by Cox regression. Model 1 controlled for age,

sex, study center, and genetic principal components, and Model 2 additionally controlled for clinical risk factors of kidney failure (baseline eGFR, prevalent diabetes, hypertension, coronary heart disease, smoking status, BMI, physical activity, education levels, and total calorie intake). We evaluated these two models combining African Americans and European Americans controlling for race by *GSTM1* homozygous deletion strata. To determine whether the association between cruciferous vegetable intake and kidney failure was stronger in those with *GSTM1* homozygous deletion, we tested for the interaction between *GSTM1* homozygous deletion and cruciferous vegetable intake. To determine whether the association between cruciferous vegetable intake and kidney failure within the *GSTM1* homozygous deletion strata differed by the two race groups, we tested for race interaction with cruciferous vegetable intake within the *GSTM1* homozygous deletion stratum.

Furthermore, we conducted three sets of secondary analyses. The first set evaluated the association between *GSTM1* deletion genotypes (*0/0, 0/1, 1/1*) and kidney failure within the three levels of cruciferous vegetable intake. The second evaluated the main effect of cruciferous vegetable intake on kidney failure. The third evaluated the main effect of *GSTM1* deletion genotype on kidney failure. The covariates of these secondary analyses were the same as the primary analysis.

All Cox regression analyses were conducted using Stata version 14. All other analyses were conducted using R.

References

1.	Salzler HR, Griffiths R, Ruiz P, Chi L, Frey C, Marchuk DA, et al. Hypertension and albuminuria in chronic kidney disease mapped to a mouse chromosome 11 locus. Kidney Int. 2007;72(10):1226-32.

2.	Ye L, Dinkova-Kostova AT, Wade KL, Zhang Y, Shapiro TA, Talalay P. Quantitative determination of dithiocarbamates in human plasma, serum, erythrocytes and urine: pharmacokinetics of broccoli sprout isothiocyanates in humans. Clin Chim Acta. 2002;316(1-2):43-53.

3.	Cechova S, Zeng Q, Billaud M, Mutchler S, Rudy CK, Straub AC, et al. Loss of collectrin, an angiotensin-converting enzyme 2 homolog, uncouples endothelial nitric oxide synthase and causes hypertension and vascular dysfunction. Circulation. 2013;128(16):1770-80.

4.	Gigliotti JC, Huang L, Ye H, Bajwa A, Chattrabhuti K, Lee S, et al. Ultrasound prevents renal ischemia-reperfusion injury by stimulating the splenic cholinergic anti-inflammatory pathway. J Am Soc Nephrol. 2013;24(9):1451-60.

5.	Cechova S, Dong F, Chan F, Kelley MJ, Ruiz P, Le TH. MYH9 E1841K Mutation Augments Proteinuria and Podocyte Injury and Migration. J Am Soc Nephrol. 2017.

6.	Sung SJ, Ge Y, Dai C, Wang H, Fu SM, Sharma R, et al. Dependence of Glomerulonephritis Induction on Novel Intraglomerular Alternatively Activated Bone Marrow-Derived Macrophages and Mac-1 and PD-L1 in Lupus-Prone NZM2328 Mice. Journal of immunology. 2017;198(7):2589-601.

7.	Cross JV, Rady JM, Foss FW, Lyons CE, Macdonald TL, Templeton DJ. Nutrient isothiocyanates covalently modify and inhibit the inflammatory cytokine macrophage migration inhibitory factor (MIF). Biochem J. 2009;423(3):315-21.

8.	Rosengren E, Bucala R, Aman P, Jacobsson L, Odh G, Metz CN, et al. The immunoregulatory mediator macrophage migration inhibitory factor (MIF) catalyzes a tautomerization reaction. Mol Med. 1996;2(1):143-9.

9.	The Atherosclerosis Risk in Communities (ARIC) Study: design and objectives. The ARIC investigators. Am J Epidemiol. 1989;129(4):687-702.

10.	Nettleton JA, Matijevic N, Follis JL, Folsom AR, Boerwinkle E. Associations between dietary patterns and flow cytometry-measured biomarkers of inflammation and cellular activation in the Atherosclerosis Risk in Communities (ARIC) Carotid Artery MRI Study. Atherosclerosis. 2010;212(1):260-7.

11.	Fawzi WW, Rifas-Shiman SL, Rich-Edwards JW, Willett WC, Gillman MW. Calibration of a semi-quantitative food frequency questionnaire in early pregnancy. Annals of epidemiology. 2004;14(10):754-62.

12.	Tang L, Paonessa JD, Zhang Y, Ambrosone CB, McCann SE. Total isothiocyanate yield from raw cruciferous vegetables commonly consumed in the United States. J Funct Foods. 2013;5(4):1996-2001.

13.	Brennan P, Hsu CC, Moullan N, Szeszenia-Dabrowska N, Lissowska J, Zaridze D, et al. Effect of cruciferous vegetables on lung cancer in patients stratified by genetic status: a mendelian randomisation approach. Lancet. 2005;366(9496):1558-60.

14.	Rebholz CM, Coresh J, Ballew SH, McMahon B, Whelton SP, Selvin E, et al. Kidney Failure and ESRD in the Atherosclerosis Risk in Communities (ARIC) Study: Comparing Ascertainment of Treated and Untreated Kidney Failure in a Cohort Study. Am J Kidney Dis. 2015;66(2):231-9.

15.	Tin A, Scharpf R, Estrella MM, Yu B, Grove ML, Chang PP, et al. The Loss of GSTM1 Associates with Kidney Failure and Heart Failure. J Am Soc Nephrol. 2017;28(11):3345-52.

16.	Jiang Y, Oldridge DA, Diskin SJ, Zhang NR. CODEX: a normalization and copy number variation detection method for whole exome sequencing. Nucleic Acids Res. 2015;43(6):e39.

17.	Carpenter CL, Yu MC, London SJ. Dietary isothiocyanates, glutathione S-transferase M1 (GSTM1), and lung cancer risk in African Americans and Caucasians from Los Angeles County, California. Nutrition and cancer. 2009;61(4):492-9.

18.   Wang LI, Giovannucci EL, Hunter D, Neuberg D, Su L, Christiani DC. Dietary intake of Cruciferous vegetables, Glutathione S-transferase (GST) polymorphisms and lung cancer risk in a Caucasian population. Cancer Causes Control. 2004;15(10):977-85.

19.   Zhao B, Seow A, Lee EJ, Poh WT, Teh M, Eng P, et al. Dietary isothiocyanates, glutathione S-transferase -M1, -T1 polymorphisms and lung cancer risk among Chinese women in Singapore. Cancer Epidemiol Biomarkers Prev. 2001;10(10):1063-7.

20.   Levey AS, Stevens LA, Schmid CH, Zhang YL, Castro AF, 3rd, Feldman HI, et al. A new equation to estimate glomerular filtration rate. Annals of internal medicine. 2009;150(9):604-12.

21.   Baecke JA, Burema J, Frijters JE. A short questionnaire for the measurement of habitual physical activity in epidemiological studies. Am J Clin Nutr. 1982;36(5):936-42.

22.   Li M, Li Y, Weeks O, Mijatovic V, Teumer A, Huffman JE, et al. SOS2 and ACP1 Loci Identified through Large-Scale Exome Chip Analysis Regulate Kidney Development and Function. J Am Soc Nephrol. 2016.

# SUPPLEMENTARY FIGURES

Supplementary Figure 1

A
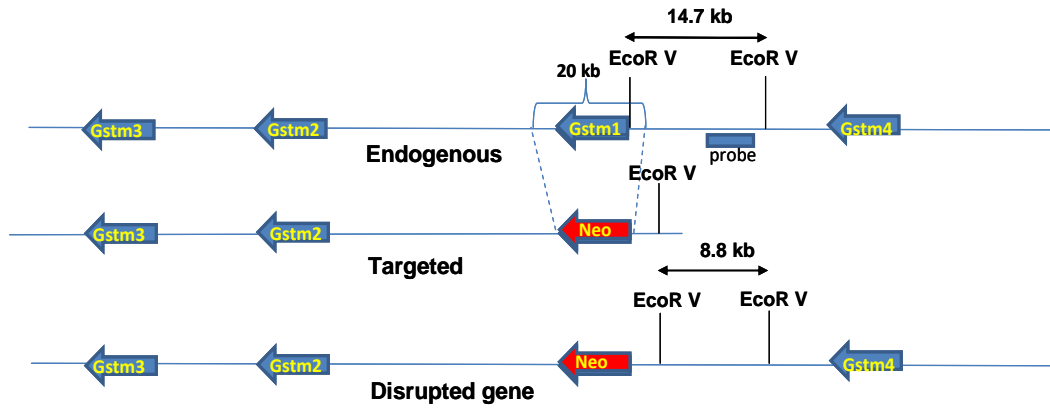
B
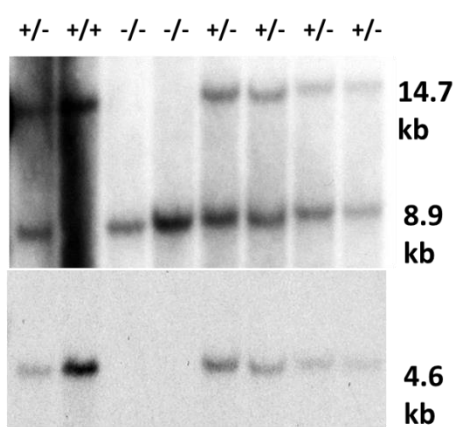

C
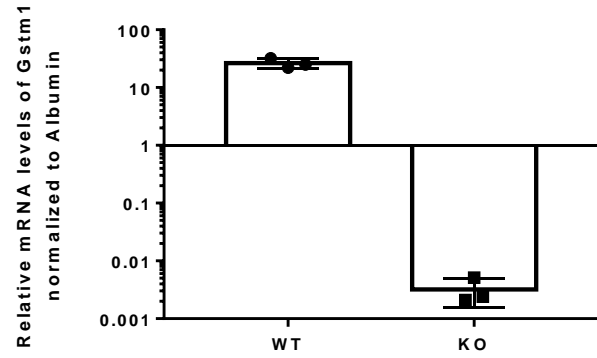
D
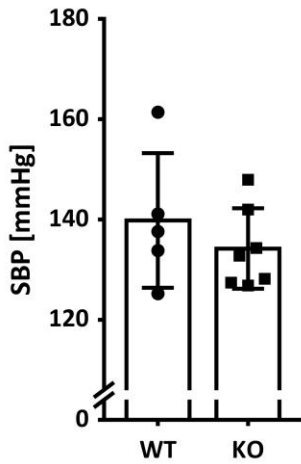
E
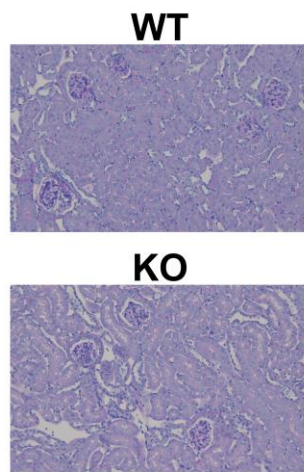
F
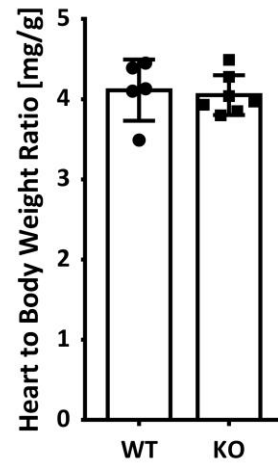
Supplementary Figure 1: Development, validation, and phenotype of 129/SvEv mice with a targeted deletion of GSTM1.

A. Scheme of the construct for deletion of the *Gstm1* gene. A 20 kb segment of the locus including the entire gene and promoter region is replaced with a selectable marker.

B. DNA of a representative litter born to parents heterozygous for Gstm1 was digested with EcoRV. **Top panel:** Using a probe outside the deleted area yielded a 14.7 kb band for WT mice (lane 2) and a 8.9 kb band for KO mice (lanes 3 and 4). Heterozygous mice showed both bands (lanes 1, 5-8). **Bottom panel:** Using a probe corresponding to the region of the locus deleted during the recombination event yielded a 4.6 kb band in WT and heterozygous that was absent in KO mice.

C. Real-time RT-PCR of *Gstm1*, normalized to a*lbumin*, confirming successful deletion in kidney tissue.

D. Systolic blood pressure (SBP) by tail cuff was not different between WT and *Gstm1* KO mice at 1 year of age (p = 0.44, n = 5/7).

E. Representative renal sections stained with PAS from 1 WT and 1 *Gstm1* KO mice showed no differences at 1 year of age.

F. Heart to body weight ratio was not different between WT and *Gstm1* KO mice at 1 year of age (p = 0.77, n = 5/7).

Supplementary Figure 2
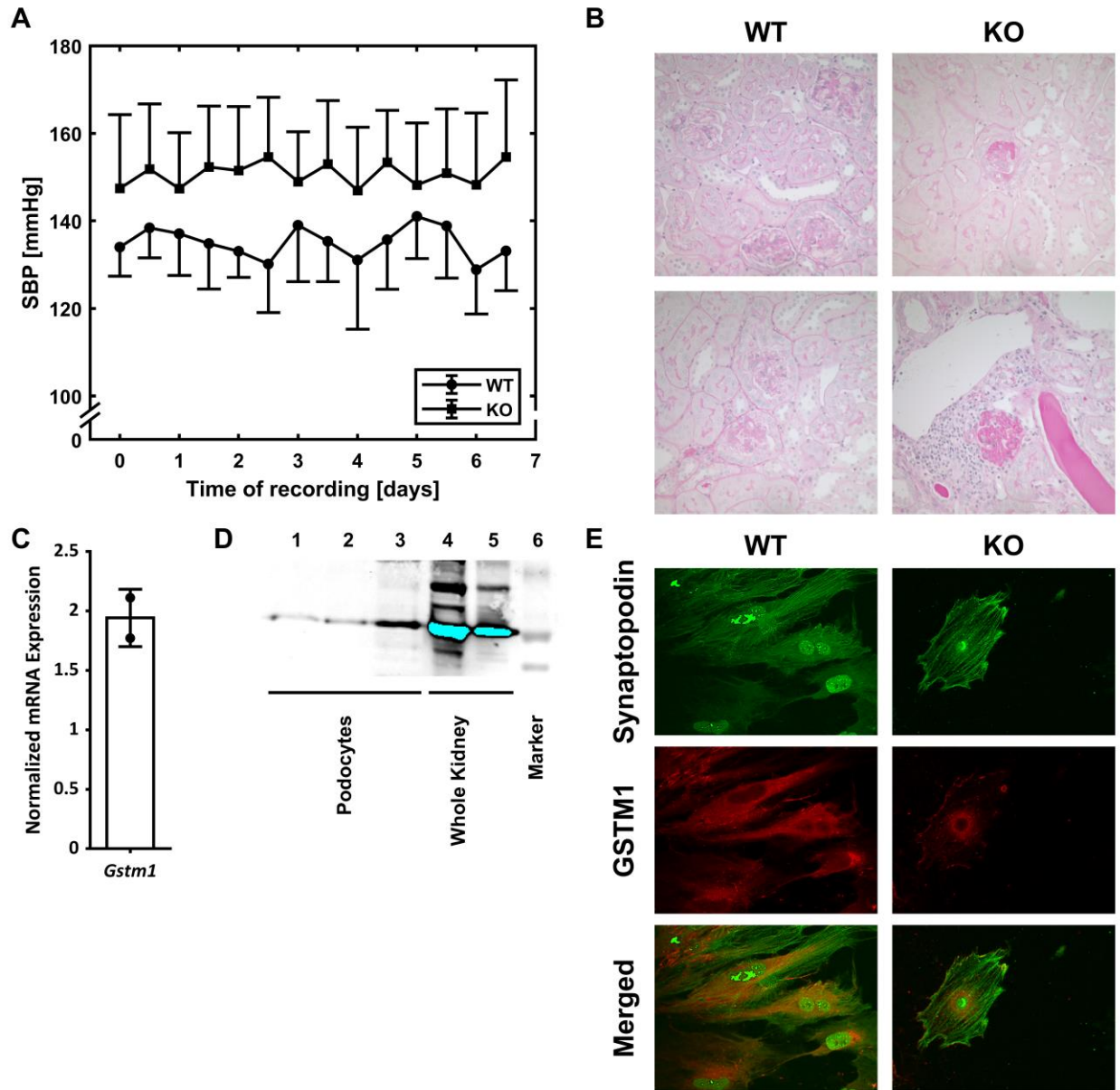
Supplementary Figure 2: Nx-CKD disease model and primary podocyte characterization.

A. Longitudinal tracing of systolic blood pressure (SBP) averaged every 12 h measured by radiotelemetry over the 1 week shown in Fig. 2B.

B. Representative renal sections stained with PAS from 2 WT and 2 KO mice 8 weeks post-Nx.

C. Real-time RT-PCR of *Gstm1* mRNA expression normalized to that of β-actin from primary podocytes isolated from the glomeruli of WT mice.

D. Western blot of GSTM1 protein. Lanes 1-3 show cell lysates from primary podocytes isolated from the glomeruli of WT mice. Lanes 4 and 5 show cell lysates from whole kidney of WT mice and are saturated (blue). Lane 6 is the ladder marker.

E. Immunostaining showing actin-associated synaptopodin protein (green, marker for podocytes) and GSTM1 (red) present in WT podocytes but abset in *Gstm1* KO podocytes.

Supplementary Figure 3

A
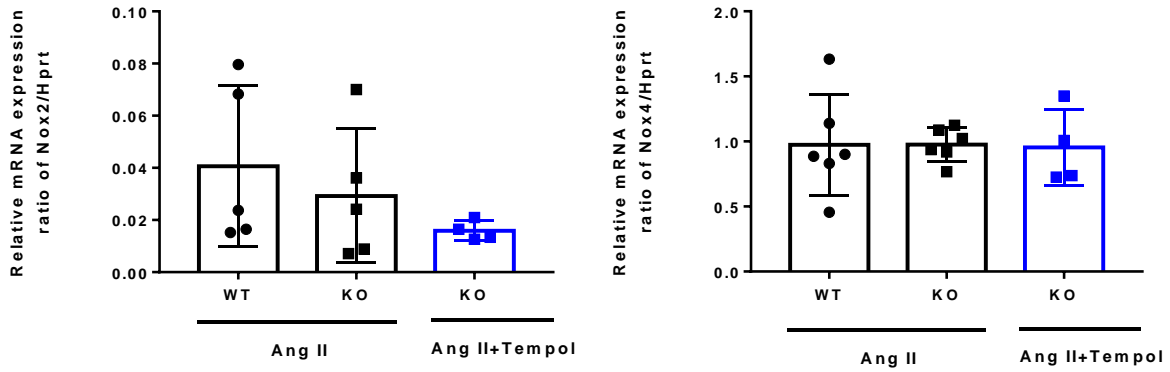
B
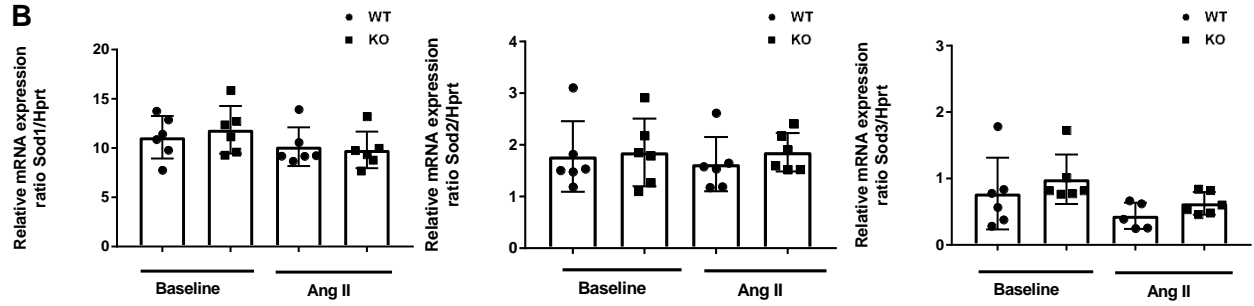
C
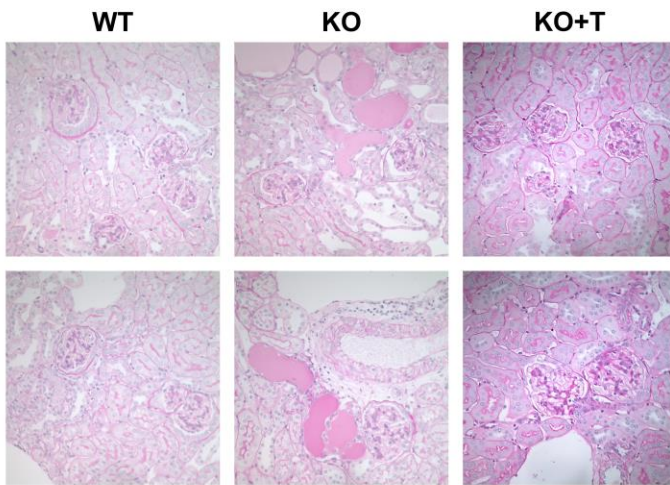
D
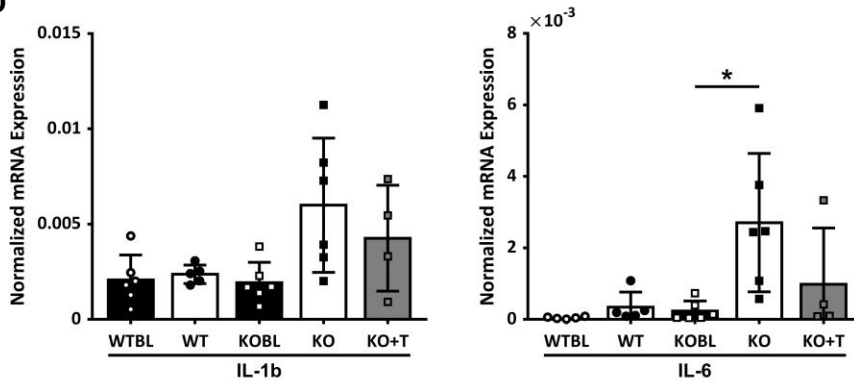
Supplementary Figure 3: Chronic AngII infusion model of hypertension.
A. Renal mRNA levels of Nox2 and Nox4 normalized to *Hprt*. Comparisons by one-way ANOVA.
B. Renal mRNA levels of *SOD* isoforms normalized to *Hprt*. Comparisons between matching WT and KO by *t*-test.
**C.** Representative renal sections stained with PAS from 2 WT and 2 KO mice after 4 weeks of AngII infusion.
D. Renal mRNA levels of additional genes involved in inflammation normalized to *Hprt* in WT mice at baseline (WTBL) and with HTN (WT), n = 6/5 and KO mice at baseline (KOBL), with HTN (KO) and with HTN treated with Tempol (KO+T), n = 6/6/4. WT comparisons by *t*-test. KO comparisons by one-way ANOVA.

Supplementary Figure 4

A

B

C
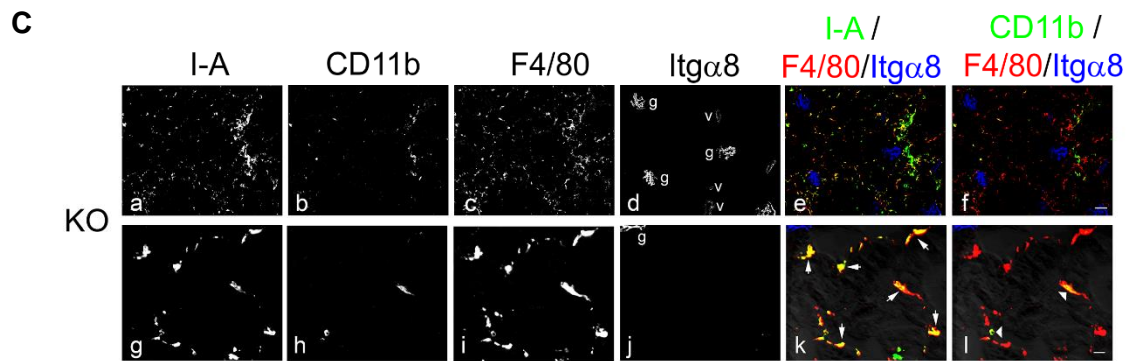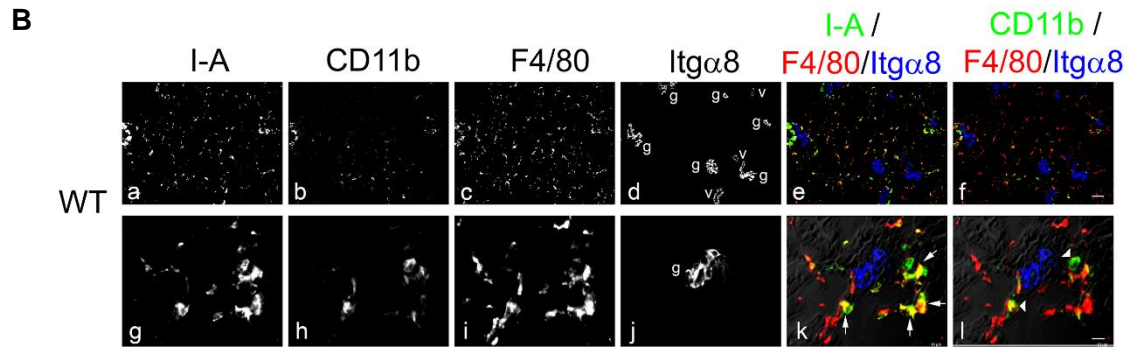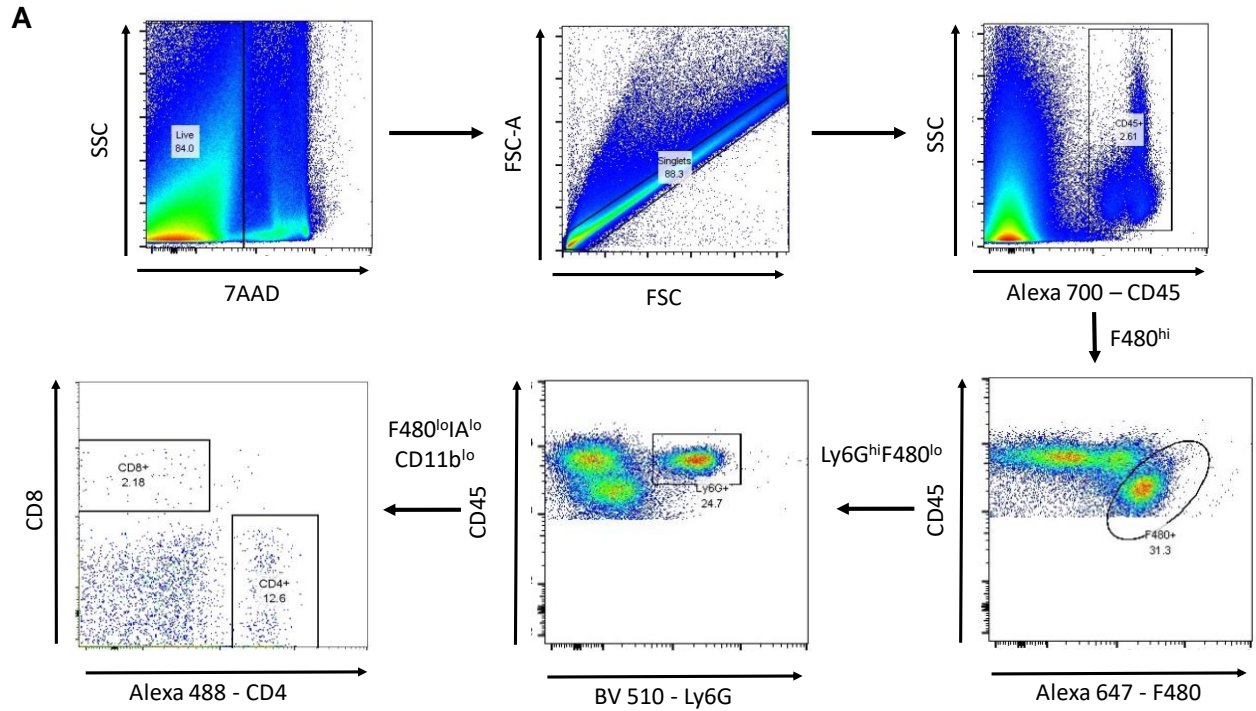
Supplementary Figure 4: Immunological analysis of kidney tissue from AngII study.
A. Representative gating strategy for quantification of renal leukocytes by flow cytometry. Live, single CD45$^+$ cells were selected based on 7AAD staining (exclusion (7AAD negative) indicates living cells) and the relationship of the width and area of forward scatter. CD45$^+$ cells were then further subdivided based on F480 and Ly6G positivity. Remaining non-myeloid cells (lacking IA, F480, and CD11b) were assessed for staining of CD4 and CD8 staining and identified as CD4$^+$ and CD8$^+$ T-cells (confirmed in separate studies by positivity for CD3$^+$).
**B.** Kidney sections from AngII-HTN WT mice were stained with the macrophage and dendritic markers I-A, CD11b and F4/80 and the mesangial cell marker integrin α8 (Itgα8). Single color (left 4 columns) and merged 3-color confocal micrographs (right 2 columns) are shown in lower (top row images a-f) and higher (bottom row images g-l) magnifications. In images d and j glomeruli (g) and blood vessels (v, Itgα8+ smooth muscle cells) are marked. In image k, arrows show interstitial F4/80$^+$I-A$^+$CD11b^{Low} cells which are largely resident renal macrophages as flow cytometry shows that the CD11c^{high}CD11b$^+$I-A$^+$ dendritic cells comprise only 6% of the CD11b$^+$ non-neutrophil populations. Interstitial resident macrophages comprising both the F4/80$^+$I-A$^{-/Low}$ (red in k) and the F4/80$^+$I-A$^+$ (yellow in k) cells are the major renal infiltrating inflammatory cell population. In image l, there are few blood-derived macrophages which are shown as CD11b^{high}F4/80^{Low} cells (arrows). Scale bars are 50 μm (image f) and 10 μm (image l).
C. Kidney sections from AngII-HTN KO mice with the same staining and markers as in B.

Supplementary Figure 5

A
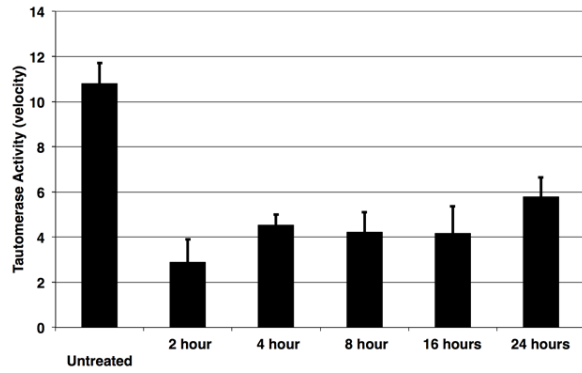
B
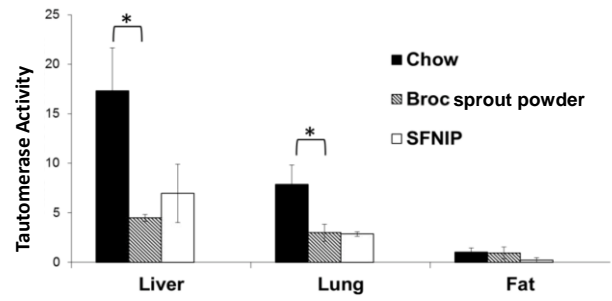
C
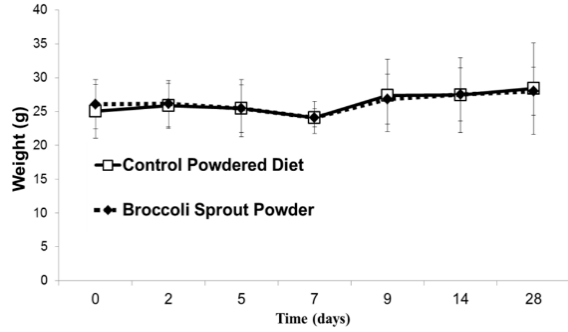
D
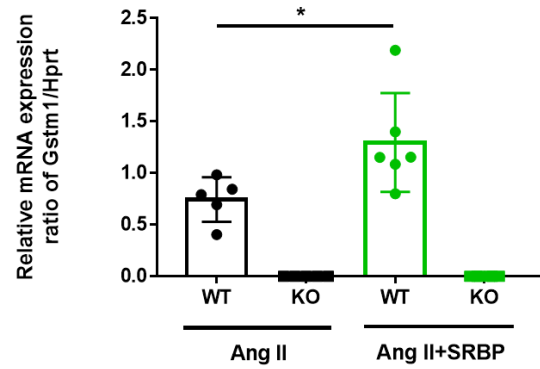
E
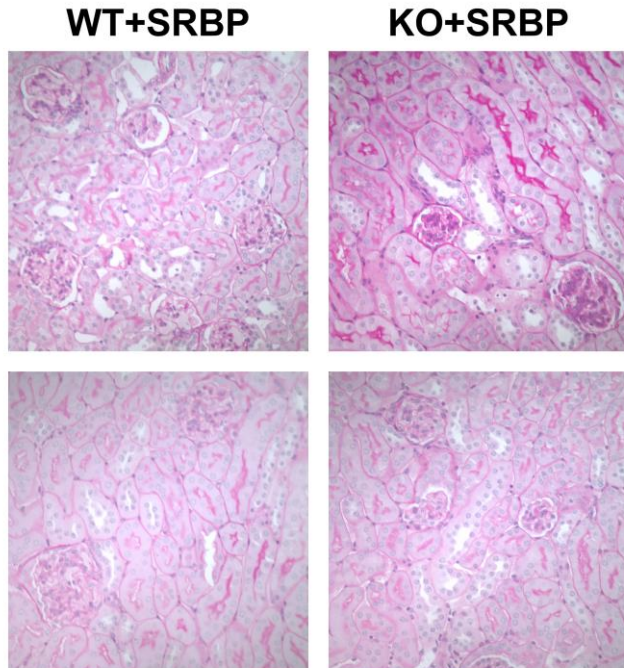
Supplementary Figure 5: Sulforaphane-Rich Broccoli Powder (SRBP) studies in vivo.
A. Pharmacodynamic data of the inhibition tautomerase activity as a surrogate for the macrophage inducible factor (MIF) activity over time by a single IP dose (2 mg) of purified sulforaphane.
B. Comparison of MIF activity by measurement of tautomerase activity between mice fed regular chow, SRBP mixed in a 1:1 ratio with regular chow, and regular chow with purified sulforaphane injected IP daily (SFNIP). * P < 0.01.
C. Body weight after 4 weeks dietary SRBP supplementation showed to difference compared to mice maintained on regular chow.
D. Measurement of *Gstm1* mRNA expression in the kidney normalized to *Hprt* showed that SRBP increased expression in WT AngII-HTN mice. As expected, KO mice showed no detectable expression on either diet. * p < 0.05.
E. Representative renal sections stained with PAS from 2 WT and 2 KO mice after 4 weeks of dietary SRBP supplementation and concurrent AngII infusion.

Supplementary Figure 6.

A. Histogram of the normalized reads at *GSTM1* by read length
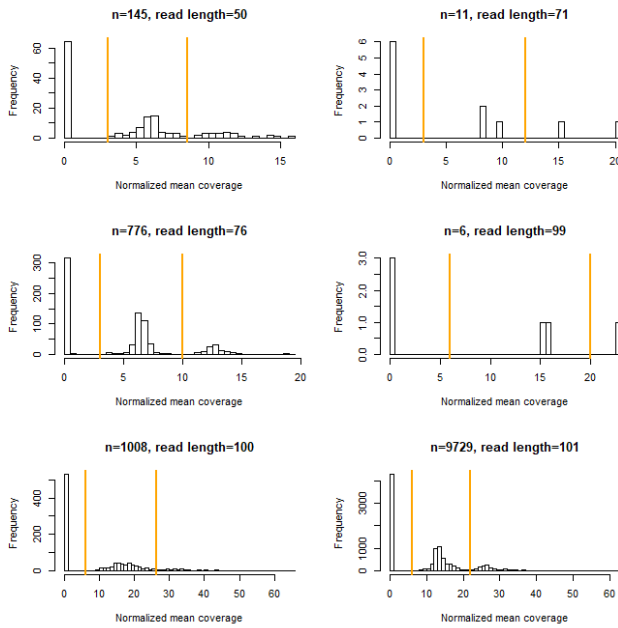
Empirical cut points by read length

Read length	Between zero and one copy	Between one copy and two copies
50	3	8.5
71	3	12
76	3	12
99	6	20
100	6	25
101	6	22

B: Density of delta-Ct Mean by plate
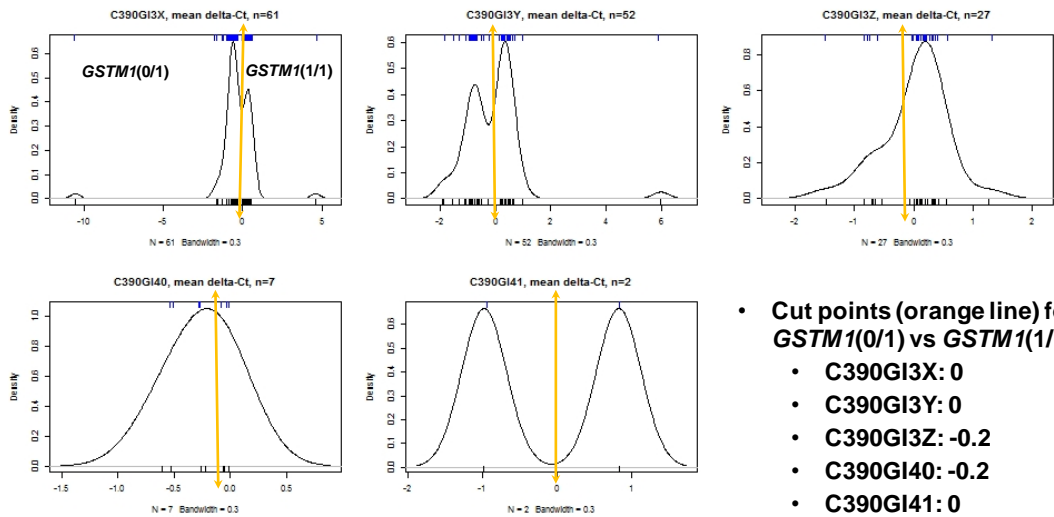
- Cut points (orange line) for *GSTM1*(0/1) vs *GSTM1*(1/1) by plate
  - C390GI3X: 0
  - C390GI3Y: 0
  - C390GI3Z: -0.2
  - C390GI40: -0.2
  - C390GI41: 0

C: Concordance of *GSTM1* deletion between qPCR and from exome sequencing reads

		Calls from Exome Sequencing Reads		
		GSTM1(0/0)	*GSTM1*(0/1)	*GSTM1*(1/1)
	GSTM1(0/0)	66	0	0
qPCR	*GSTM1*(0/1)	0	67	7
	GSTM1(0/1)	0	8	64

Supplementary Figure 6: Genotyping for *GSTM1* in ARIC cohort
A. Histogram of the normalized exome sequencing reads at *GSTM1* by read length.
B. Density of mean ΔCt (*GSTM1* vs *RPPH1*) by plate in real-time PCR (qPCR) experiments validating exome sequencing call of *GSTM1* deletion.
C. Concordance of *GSTM1* deletion call between real-time PCR (qPCR) experiments and the algorithm using exome sequencing reads (n = 212).

Supplementary Table 1. Previous sub-sample and additional participants by cruciferous vegetable intake category, n (%)

	Low intake	Medium intake	High intake	Total
Previous sub-sample	1,174 (21.5)	3,084 (56.5)	1,203 (22.0)	5461 (100)
Additional participants	843 (18.0)	2,596 (55.3)	1,255 (26.7)	4694 (100)

Previous sub-sample was used in Tin et al. JASN 2016

Supplementary Table 2. Frequency of GSTM1 deletion genotype frequency in ARIC, n (%)

	Homozygous deletion (0/0)	Hemizygous deletion (0/0)	No deletion (1/1)	Total
African American	707 (26.1)	1310 (48.3)	696 (25.7)	2713
European American	3894 (52.3)	2940 (39.5)	608 (8.2)	7442

Supplementary Table 3. Association between cruciferous vegetable intake and kidney failure within each *GSTM1* genotype

Hazard ratio (95% confidence interval)			
	Low intake	Medium intake	High intake	p-trend
Model 1				
GSTM1(0/0)	Reference	0.58 (0.41, 0.82)	0.41 (0.25, 0.68)	<0.0001
GSTM1(0/1)	Reference	0.83 (0.57, 1.22)	0.95 (0.59, 1.53)	0.79
GSTM1(1/1)	Reference	0.50 (0.26, 0.96)	0.75 (0.33, 1.71)	0.30
Model 2				
GSTM1(0/0)	Reference	0.68 (0.48, 0.98)	0.49 (0.29, 0.83)	0.005
GSTM1(0/1)	Reference	0.78 (0.53, 1.15)	0.93 (0.57, 1.53)	0.73
GSTM1(1/1)	Reference	0.46 (0.23, 0.93)	0.83 (0.35, 1.98)	0.42

Model 1 covariates: age, sex, race, center, genetic principal components
Model 2: Model 1 + eGFR, prevalent diabetes, hypertenion, and coronary heart disease, smoking status, BMI, leisure physical activity, education levels, and total calorie intake.
N (event). GSTM1(0/0) 4,601 (159); GSTM1(0/1): 4,250 (163); GSTM1(1/1): 1,304 (48)

Supplementary Table 4. Association between cruciferous vegetable intake and kidney failure by GSTM1 homozygous deletion in the two race groups

	Hazard ratio (95% confidence interval)			
	Low	Medium	High	p-trend
African Americans				
Model 1				
GSTM1(0/0)	Reference	0.55 (0.31, 0.96)	0.48 (0.20, 1.15)	0.04
GSTM1(0/1 or 1/1)	Reference	0.88 (0.59, 1.31)	0.86 (0.48, 1.52)	0.54
Model 2				
GSTM1(0/0)	Reference	0.67 (0.37, 1.23)	0.49 (0.20, 1.24)	0.1
GSTM1(0/1 or 1/1)	Reference	0.81 (0.54, 1.23)	0.75 (0.41, 1.37)	0.3
European Americans				
Model 1				
GSTM1(0/0)	Reference	0.60 (0.38, 0.93)	0.38 (0.21, 0.71)	0.002
GSTM1(0/1 or 1/1)	Reference	0.56 (0.31, 0.95)	0.85 (0.47, 1.54)	0.77
Model 2				
GSTM1(0/0)	Reference	0.63 (0.40, 0.99)	0.42 (0.22, 0.78)	0.005
GSTM1(0/1 or 1/1)	Reference	0.54 (0.31, 0.95)	1.13 (0.61, 2.11)	0.59

P-value for interaction between GSTM1 deletion and cruciferous vegetable intake:
European Americans: Model 1: 0.06, Model 2: 0.01
African Americans > 0.05

Model 1 covariates: age, sex, center, genetic principal components
Model 2: Model 1 + eGFR, prevalent diabetes, hypertenion, and coronary heart disease, smoking status, BMI, leisure physical activity, education levels, and total calorie intake.

Supplementary Table 5. Association between GSTM1 homozgyous deletion and kidney failure within each cruciferous vegetable intake category

	Hazard ratio (95% confidence interval)		
	GSTM1(0/0)	*GSTM1*(0/1 or 1/1)	P-value
Low intake			
Model 1	1.52 (1.03, 2.25)	Reference	0.04
Model 2	1.12 (0.76, 1.66)	Reference	0.56
Medium intake			
Model 1	1.27 (0.94, 1.71)	Reference	0.12
Model 2	1.25 (0.92, 1.69)	Reference	0.16
High intake			
Model 1	0.68 (0.41, 1.13)	Reference	0.14
Model 2	0.60 (0.35, 1.02)	Reference	0.06

Model 1 covariates: age, sex, race, center, genetic principal components
Model 2: Model 1 + eGFR, prevalent diabetes, hypertenion, and coronary heart disease, smoking status, BMI, leisure physical activity, education levels, and total calorie intake

Supplementary Table 6. Association between the three GSTM1 deletion genotypes and kidney failure within each cruciferous vegetable intake category

	Hazard ratio (95% confidence interval)			
	GSTM1(0/0)	*GSTM1*(0/1)	*GSTM1*(1/1)	p-trend
Low intake				
Model 1	1.60 (0.91, 2.81)	1.08 (0.61, 1.90)	Reference	0.06
Model 2	1.18 (0.67, 2.07)	1.07 (0.60, 1.91)	Reference	0.54
Medium intake				
Model 1	2.01 (1.21, 3.33)	1.79 (1.10, 2.92)	Reference	0.01
Model 2	1.82 (1.09, 3.02)	1.60 (0.98, 2.62)	Reference	0.03
High intake				
Model 1	0.79 (0.36, 1.70)	1.21 (0.59, 2.46)	Reference	0.31
Model 2	0.63 (0.28, 1.42)	1.07 (0.51, 2.26)	Reference	0.12

Model 1 covariates: age, sex, race, center, genetic principal components
Model 2: Model 1 + eGFR, prevalent diabetes, hypertenion, and coronary heart disease, smoking status, BMI, leisure physical activity, education levels, and total calorie intake.

Supplementary Table 7. Overall association between cruciferous vegetable intake and kidney failure

	Low intake	Medium intake	High intake	p-trend
Hazard ratio (95% confidence interval)				
African American				
Model 1	Reference	0.75 (0.54, 1.03)	0.72 (0.45, 1.16)	0.10
Model 2	Reference	0.78 (0.56, 1.08)	0.70 (0.43, 1.14)	0.11
European American				
Model 1	Reference	0.58 (0.41, 0.82)	0.58 (0.38, 0.88)	0.01
Model 2	Reference	0.59 (0.41, 0.84)	0.69 (0.45, 1.05)	0.08
Combined				
Model 1	Reference	0.66 (0.52, 0.83)	0.64 (0.47, 0.87)	0.002
Model 2	Reference	0.68 (0.53, 0.86)	0.70 (0.51, 0.96)	0.01

Model 1 covariates: age, sex, center, genetic principal components
Model 2: Model 1 + eGFR, prevalent diabetes, hypertenion, and coronary heart disease, smoking status, BMI, leisure physical activity, education levels, and total calorie intake.

In the race combined analysis, race was included as a covariate

Supplementary Table 8. Overall association between *GSTM1* deletion genotype and kidney failure (recessive model)

	Hazard ratio (95% confidence interval)		
	GSTM1(0/0)	*GSTM1*(0/1 or 1/1)	p-value
African American			
Model 1	1.30 (0.95, 1.78)	Reference	0.10
Model 2	1.21 (0.88, 1.66)	Reference	0.24
European American			
Model 1	1.14 (0.85, 1.52)	Reference	0.39
Model 2	1.06 (0.79, 1.42)	Reference	0.72
Race combined			
Model 1	1.21 (0.98, 1.50)	Reference	0.08
Model 2	1.10 (0.88, 1.36)	Reference	0.4

Model 1 covariates: age, sex, center, genetic principal components
Model 2: Model 1 + eGFR, prevalent diabetes, hypertenion, and coronary heart disease, smoking status, BMI, leisure physical activity, education levels, and total calorie intake.

In the race combined analysis, race was included as a covariate

Supplementary Table 9. Overall association between GSTM1 deletion and kidney failure (genotypic model)

	Hazard ratio (95% confidence interval)			p-trend
	GSTM1(0/0)	*GSTM1*(0/1)	*GSTM1*(1/1)	
African American				
Model 1	1.68 (1.11, 2.56)	1.45 (0.99, 2.13)	Reference	0.02
Model 2	1.42 (0.93, 2.17)	1.26 (0.85, 1.85)	Reference	0.11
European American				
Model 1	1.35 (0.74, 2.46)	1.23 (0.66, 2.26)	Reference	0.3
Model 2	1.31 (0.71, 2.39)	1.29 (0.69, 2.40)	Reference	0.52
Race combined				
Model 1	1.57 (1.12, 2.19)	1.39 (1.01, 1.93)	Reference	0.01
Model 2	1.30 (0.92, 1.82)	1.24 (0.89, 1.72)	Reference	0.18

Model 1 covariates: age, sex, center, genetic principal components
Model 2: Model 1 + eGFR, prevalent diabetes, hypertenion, and coronary heart disease, smoking status, BMI, leisure physical activity, education levels, and total calorie intake.

In the race combined analysis, race was included as a covariate

Supplementary Table 10. Response categories of cruciferous vegetable intake in food frequency questionarie (per 0.5 cup)

> 6 per day
4-6 per day
2-3 per day
1 per day
5-6 per week
2-4 per week
1 per week
1-3 per month
Almost never

Supplementary Table 11. N (kidney failure events) by race, GSTM1 deletion, and cruciferous vegetable intake categories

	Low intake	Medium intake	High intake
African Americans			
GSTM1(0/0)	180 (23)	400 (28)	127 (7)
GSTM1(0/1 or 1/1)	520 (36)	1182 (75)	304 (19)
European Americans			
GSTM1(0/0)	704 (31)	2157 (54)	1033 (16)
GSTM1(0/1 or 1/1)	613 (21)	1941 (34)	994 (26)

Supplementary Table 12. Sequences of Primers for RT-PCR		
Gene	Forward Primer	Reverse Primer
Hprt	CAAACTTTGCTTTCCCTGGT	CAAGGGCATATCCAACAACA
Gstm1	CCTATGATACTGGGATACTGGAACG	GGAGCGTCACCCATGGTG
Nox2	GTGCACCATGATGAGGAGAA	AGTTTCAGCCAAGGCTTCAG
Nox4	CAGTCAAACAGATGGGATTCA	GAACTGGGTCCACAGCAGA
CXCL1	ACCGAAGTCATAGCCACACTC	ACAGGTGCCATCAGAGCAGT
MCP1	ACCTGCTGCTACTCATTCACC	CCATTCCTTCTTGGGGTCAG
IL-1β	TGTCCTGTGTAATGAAAGACG	TGCTTGTGAGGTGCTGATGT
IL-6	CAGAGTCCTTCAGAGAGATACAGAAAC	TGGATGGTCTTGGTCCTTAGC
IL-17α	GCCCTCAGACTACCTCAACC	AGCTTCCCAGATCACAGAGG
Sod1	AACCAGTTGTGTTGTCAGGAC	CCACCATGTTTCTTAGAGTGAG
Sod2	CAGACCTGCCTTACGACTATGG	CTCGGTGGCGTTGAGATTGTT
Sod3	CCTTCTTGTTCTACGGCTTGC	TCGCCTATCTTCTCAACCAG